ARTICLE
Journal of Cellular Biochemistry 117:94–105 (2016)

Journal of Cellular Biochemistry

A Novel Danshensu Derivative Prevents Cardiac Dysfunction and Improves the Chemotherapeutic Efficacy of Doxorubicin in Breast Cancer Cells

Liang Wang,[1,2] Xiaojing Zhang,[3] Judy Yuet-Wa Chan,[1] Luchen Shan,[3]* Guozhen Cui,[1] Qingbin Cui,[3] Yingfei Wang,[3] Jingjing Li,[1] Huanxian Chen,[1] Qingwen Zhang,[1] Pei Yu,[3] Yifan Han,[2] Yuqiang Wang,[3] and Simon Ming-Yuen Lee[1]**

[1]*State Key Laboratory of Quality Research in Chinese Institute of Chinese Medical Sciences, University of Macau, Macao, China*

[2]*Department of Applied Biology and Chemical Technology, Institute of Modern Medicine, Hong Kong Polytechnic University, Hong Kong, China*

[3]*Institute of New Drug Research, College of Pharmacy, Jinan University, Guangzhou, China*

ABSTRACT

Doxorubicin (Dox) is an anthracycline antibiotic widely used in clinics as an anticancer agent. However, the use of Dox is limited by its cardiotoxicity. We have previously shown that a Danshensu (DSS) derivative, ADTM, displayed strong cardioprotective effects. With improved chemical stability and activity, a novel DSS derivative, D006, based on the structure of ADTM, was synthesized. In the present study, the protective effects of D006, indexed by attenuation of the cardiotoxicity induced by Dox as well as chemosensitizing effects that increase the antitumor activity of Dox, were investigated. Our results showed that D006 was more potent than either parental compound, or their use in combination, in ameliorating Dox-induced toxicity in H9c2 cells. In our zebrafish model, D006, but not DSS, alone significantly preserved the ventricular function of zebrafish after Dox treatment. Moreover, D006 upregulated mitochondrial biogenesis and increased mtDNA copy number after Dox treatment of H9c2 cells. D006 promoted the expression of HO-1 protein in a time-dependent manner while the HO-1 inhibitor, Znpp, reversed the protective effects of D006. In human breast tumor MCF-7 cells, D006 enhanced Dox-induced cytotoxicity by increasing apoptosis. In conclusion, our results indicate that a new DSS derivative exhibits promising protective effects against Dox-induced cardiotoxicity both in vivo and in vitro, an effect at least partially mediated by induction of HO-1 expression and the activation of mitochondrial biogenesis. Meanwhile, D006 also potentiated the anti-cancer effects of Dox in breast tumor cells. J. Cell. Biochem. 117: 94–105, 2016.

KEY WORDS: DOXORUBICIN; MITOCHONDRIAL BIOGENESIS; CARDIOTOXICITY; BREAST CANCER

Doxorubicin (Dox), which is widely used to treat a variety of tumors including breast cancer, hematological malignancies and soft tissue sarcomas, may cause serious cardiotoxicity [Suliman et al., 2007a]. In a retrospective analysis by Von Hoff et al. [1979] the incidence of congestive heart failure in clinics was 7.5 and 18% when patients were administered cumulative doxorubicin doses of 550 mg/m^2 and 700 mg/m^2, respectively. A more recent report, showed that 26% of patients would suffer from congestive heart failure at cumulative Dox doses of 550 mg/m^2 [Swain et al., 2003]. Because of this increase in irreversible congestive heart failure, it is recommended that cumulative doxorubicin doses should not exceed 550 mg/m^2 [Feenstra et al., 1999; Misset et al., 1999].

Recent studies showed that suppressed cardiac mitochondrial biogenesis and upregulated mtDNA damage may play vital roles in the pathogenesis of Dox-induced cardiomyopathy [Zhou et al., 2001; Miyagawa et al., 2010]. The peroxisome proliferator–activated

Liang Wang and Xiaojing Zhang contribute equally to this work.

Conflict of interest: None

Grant sponsor: Research Committee of University of Macau; Grant number: MYRG138(Y1-L4)-ICMS12-LMY; Grant sponsor: The Hong Kong Polytechnic University; Grant number: G-SB10.

*Correspondence to: Luchen Shan, Institute of New Drug Research, College of Pharmacy, Jinan University, Guangzhou, China. E-mail: ytysxs@126.com

**Correspondence to: Simon Ming-Yuen Lee, Institute of Chinese Medical Sciences, Room 7003, N22 Building, University of Macau, Avenide da Universidade, Taipa, Macau, China. E-mail: simonlee@umac.mo

Manuscript Received: 22 April 2015; Manuscript Accepted: 5 June 2015

Accepted manuscript online in Wiley Online Library (wileyonlinelibrary.com): 8 June 2015

DOI 10.1002/jcb.25253 • © 2015 Wiley Periodicals, Inc.

receptor-gamma coactivator-1 family members PGC-1α and β, which exhibit strong homology among the PGC-1 family, are mainly present in the heart and skeletal muscles and play a key role in regulating mitochondrial biogenesis as well as in maintaining mitochondrial energy metabolism [Wareski et al., 2009]. Mitochondrial biogenesis requires mtDNA replication and expression, which depend on PGC-1α and β, transcription factors including nuclear respiratory factors (NRFs), estrogen-related receptors (ERRs), and mitochondrial transcription factors A (Tfam).

Dexrazoxane, an iron chelator, is the only drug currently approved by the FDA that provides cardioprotection against Dox-induced cardiotoxicity [Swain and Vici, 2004]. However, dexrazoxane not only produced side effects, such as hematological toxicity and myelosuppression, but also decreased the anti-tumor efficacy of Dox [Gharib and Burnett, 2002; Sun et al., 2013a]. Therefore, it is important to develop a drug that confers cardioprotection during doxorubicin treatment and improves the chemotherapeutic efficacy of doxorubicin in cancer cells.

Our previous studies revealed that the danshensu (DSS) and tetramethylpyrazine (TMP) derivative ADTM showed strong cardioprotective effects both in vitro and in vivo through the Akt/PI3K and Nrf2/HO-1 pathways [Cui et al., 2013]. However, further study indicated that the protective effect of ADTM, against Dox-induced cardiotoxicity, was not potent in H9c2 cells. Accumulating evidence indicates that H_2S exhibits cardioprotective effects against hypoxia-induced cell death in H9c2 cells, myocardial ischemia in vivo and Dox-induced cardiotoxicity, and also inhibits isoproterenol and hyperhocysteinemia-induced myocardial injury in vivo [Calvert et al., 2009; Guo et al., 2013a; Guo et al., 2013b]. The H_2S donor 4-(3-thioxo-3H-1, 2-dithiol-4-yl)-benzoic acid (ACS) was developed to maintain sulfide levels in biological fluid and slow the release of H_2S into the circulation [Marutani et al., 2012]. Based on these studies, we hypothesized that a hybrid compound consisting of ADTM and ACS would be more effective than ADTM or ACS alone with respect to conferring cardioprotection. In this study, another DSS derivative, D006, was also synthesized to increase the potency and chemical stability of ADTM. D006 is a high sterically hindered derivative, derived from danshensu (DSS), which couples with tetramethylpyrizine (TMP) and ACS (Fig. 1). We found that D006 exhibited strong cardioprotective activity against doxorubicin toxicity both in vitro and in vivo. Our data indicates that the protective effects of D006 were at least partly mediated by HO-1 and mitochondrial biogenesis. D006 also enhanced the chemotherapeutic efficacy of doxorubicin in breast cancer cells.

METHODS

MATERIALS

ACS and D006 were synthesized at Jinan University, China. TMP, DSS were purchased from Shanghai Banghai Chemical Company (China) and Xi′an Honson Biotechnology (China). The purity of ACS and D006 used in the present study were >98 and >93%, respectively. D006 was prepared in a 30 mM stock solution in DMSO. Fetal bovine serum (FBS), Dulbecco′s Modified Eagle′s Medium (DMEM), penicillin and streptomycin were purchased from Gibco Life Technologies (USA). 3-(4, 5-dimethylthiazol-2-yl)-2, 5-diphenyltetrazoliumbromide (MTT) and HO-1 inhibitor zinc protoporphyrin (Znpp) were purchased from Sigma-Aldrich (USA). The Cytotoxicity Detection Kit was purchased from Roche Applied Science (Germany). 2′, 7′-dichlorofluorescein diacetate (DCFH-DA) was purchased from Invitrogen (USA).

ANIMALS

Tg(*cmlc2*: GFP) zebrafish with GFP specifically expressed in the myocardial cells were used in this study [Huang et al., 2003]. Zebrafish were maintained as described in the Zebrafish Handbook.

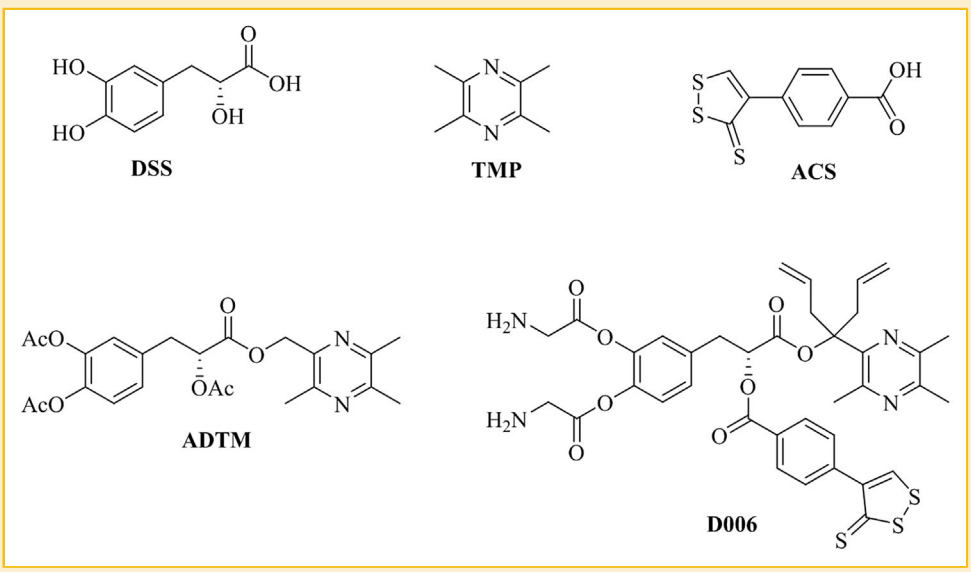

Fig. 1. Chemical structures of DSS, TMP, ACS, ADTM and D006. ADTM is synthesized by coupling DSS and TMP. D006 is a high sterically hindered derivative, derived from DSS, which couples with TMP and ACS.

Adult fish were raised at 26–28°C in aquaculture system on a 12 h:12 h (light:dark) cycle, and fed twice daily with newly hatched brine shrimp. All animal experiments were conducted according to the ethical guideline approved by Institute of Chinese Medical Sciences, the University of Macau.

EMBRYO COLLECTION AND DRUG TREATMENT

Zebrafish embryos were prepared as previously described [Tang et al., 2010]. Briefly, pair-wise mating (3–12 months old) was used to generate the zebrafish embryos which were maintained in embryo medium at 28.5°C. All embryos were then raised in the embryo medium containing 1-phenyl-2-thiourea (200 μM) after 24 hpf. Zebrafish (2 dpf) at the same developmental stage were distributed into a 12-well microplate (12–15 fish per well). After co-treatment with Dox and different concentrations of D006 or DSS for 32 h, ventricular functions of zebrafish were examined by assessing various parameters and morphology.

MEASUREMENT OF MORPHOLOGY AND FUNCTIONS OF ZEBRAFISH HEART

The morphology and functions of zebrafish heart were measured by Cellˆ R imaging system comprising IX71 microscope (Olympus). Zebrafish were placed into 1% low melting point agarose (Gibco) to restrict their movement and the movies of zebrafish heartbeat were recorded for 10 s (13–15 frames per second) at the room temperature. The parameters and morphology of ventricular function of zebrafish were measured as previously described [Ding et al., 2011; Huang et al., 2011; Zhang et al., 2012]. The volume of ventricle was calculated using the formula for a prolate spheroid: $V = 4/3\pi ab^2$. In the formula, the longitudinal axis was represented by a while the lateral axis was represented by b. Stroke volume, cardiac output and percentage of fractional shortening (% FS) of ventricle were measured using the following formulas, respectively. Stroke volume was calculated by end diastolic volume-end systolic volume. Cardiac output was determined by heart rate × stroke volume. Percentage of fractional shortening (% FS) was calculated by the difference between diastolic diameter and systolic diameter divided by diastolic diameter.

CELL CULTURES

H9c2 cells were cultured in DMEM medium supplemented with 100 IU ml^{-1} penicillin-streptomycin and 10% fetal bovine serum at 37°C in a humidified incubator containing 5% CO_2. The cells were used until they reached 70–80% confluence. H9c2 cells were differentiated with 10 nM of retinoic acid for 7 days in DMEM medium containing 0.5% FBS.

MEASUREMENT OF LACTATE DEHYDROGENASE (LDH) ACTIVITY, CELL VIABILITY AND ATP LEVEL

Cytotoxicity and cell viability of H9c2 cells were detected by LDH assay, MTT. Briefly, H9c2 cells were seeded into 96-well plates at 1×10^4 cells/well for 24 h and then exposed to 1 μM doxorubicin with or without various concentrations of D006 for another 24 h. For cytotoxicity assay, the release of LDH into the medium was determined using a Cytotoxicity Detection Kit. The absorbance was measured with a microplate reader at 490 nm. LDH release was expressed as the percentage of total LDH and the result was shown as a percentage relative to corresponding controls. Cell viability was measured by MTT assay. For MTT assay, after appropriate treatment, H9c2 cells were incubated for 4 h at 37°C in MTT solution (1 mg/ml). Then, the purple formazan was dissolved in 100 μl DMSO. The absorbance was read at 570 nm using microplate reader. ATP assay was performed to measure cellular ATP levels according to the manufacturer's protocol (CellTiter-Glo luminescent cell viability assay, Promega).

ASSESSMENT OF CELL MORPHOLOGY

Cell morphology of H9c2 cells was assessed by F-actin staining. Briefly, H9c2 cells were cultured in 96-well plates for 24 h. After 24 h of treatment with Dox in the presence or absence of D006, the cells were fixed with 4% PFA for 15 min at room temperature. After fixation, the cells were permeabilized by PBS containing 0.2% Triton for 30 min. F-actin in cells was stained with Rhodamine Phalloidin (Life Technologies) for another 1 h and then incubated with DAPI for 5 min to label nuclear DNA. The representative images of F-actin were visualized by In Cell Analyzer 2000 system.

HOECHST 33342 STAINING

Hoechst 33342 staining was used to analyze the apoptotic cells. Briefly, cells were cultured in 96 well plates for 24 h. After 24 h of treatment with Dox in the presence or absence of D006, the cells were incubated with Hoechst 33342 for another 15 min at 37°C. The apoptotic cells with changes in chromatin condensation were then visualized by In Cell Analyzer 2000 system. The apoptotic cells were analyzed using Developer Toolbox software and calculated as: apoptotic cells/total cells counted × 100%. At least 16 fields of each group were observed and counted.

MEASUREMENT OF INTRACELLULAR ROS

After 24 h of Dox treatment with or without D006, H9c2 or MCF-7cells were loaded with 10 μM DCFH-DA in medium for 30 min at 37°C. After incubation, the cells were washed with PBS and then intracellular ROS level was measured using In Cell Analyzer 2000 system. The total cell numbers and ROS positive cells were analyzed using Developer Toolbox software. At least 16 fields of each group were observed and counted.

CASPASE-3 ACTIVITY ASSAY

The activity of caspase-3 was determined using Caspase-3 Activity Assay (Life Technologies). Briefly, the cells were cultured in six well plates for 24 h. After 24 h of Dox treatment in the presence or absence of D006, H9c2 cells were harvested and the activity of caspase-3 was measured using Caspase-3 assay kit according to the protocol provided by the manufacturer.

REAL-TIME QUANTITATIVE POLYMERASE CHAIN REACTION

Total RNA from H9c2 cells was extracted using the RNeasy Mini Kit (Qiagen) according to the manual's instruction. Real-time quantitative polymerase chain reaction (PCR) was then used to analyze the mRNA expression of PGC-1β, Nrf-1 and Tfam. The primers for the PCR were as follows: PGC-1β (forward, 5′-ttgacagtggagctttgtgg-3′; reverse,

5′-gggcttatatggaggtgtgg-3′), PGC-1α (forward, 5′-aaagggccaagcagagaga-3′; reverse, 5′-gtaaatcacacggcgctctt-3), Tfam (forward, 5′-agctaaacacccagatgcaaa-3′; reverse, 5′-tcagctttaaaatccgcttca-3′).

WESTERN BLOT ANALYSIS

Whole cell lysate was prepared as described previously [Cui et al., 2013]. Briefly, cells were washed with PBS for three times and lysed with lysis buffer (RAPI containing with 1% phenylmethanesulfonyl fluoride and 1% protease inhibitor cocktail). After incubation on ice for 30 min, the lysates were centrifuged at 12,500*g* for 20 min at 4°C. The concentration of supernatant protein was determined by BCA protein assay. Protein sample was then denatured at 95°C for 5 min, separated by SDS-PAGE (sodium dodecyl sulfate polyacrylamide gel electrophpresis) and then transferred to FVDF (polyvinylidene fluoride) membrane. The membrane was incubated with the primary antibodies against PGC-1α, NRF-1 and Nrf-2 (Santa Cruz Biotechnology Inc.); β-actin, cleaved-caspase 9, cleaved-PARP, cleaved-caspase 7, p53, p-p53 (Cell Signaling) and HO-1(Abcam) overnight at 4°C, respectively. Then, the membrane was washed and incubated with secondary horseradish peroxidase-conjugated goat anti-rabbit or anti-mouse antibodies (Cell Signaling). Finally, the blots were developed with Enhanced ECL System (GE Healthcare) and the signal was quantified by Quantity One software (BioRad) (Fig. 1).

MEASUREMENT OF MITOCHONDRIAL DNA (mtDNA) LEVEL

Total cellular DNA was extracted from H9c2 cells using QlAamp DNA kit (Qiagen, Germany). Mitochondrial DNA was determined by real-time PCR using 18S rRNA primers (forward: 5′-TCAAGAACGAAAGTCGGAGG-3′; reverse: 5′-GGACATCTAAGGGCATCACA-3′) for a nuclear target sequence and D-loop primers (forward: 5′-GGTTCTTACTTCAGGGCCATCA-3′; reverse: 5′-GATTAGACCCGTTACCATCGAGAT-3′) for the mtDNA target sequence. The amount of mtDNA will be calculated by real-time PCR.

STATISTICAL ANALYSIS

Data were presented as mean ± standard deviation (SD). Differences between the groups were compared by One-way ANOVA followed by Turkey's multiple comparison tests. *P* values less than 0.05 were considered as statistically significant.

RESULTS

D006 ATTENUATED DOXORUBICIN-INDUCED CARDIOTOXICITY IN H9c2 CELLS

As shown in Figure 2A, treatment with D006 alone for 24 h was not associated with cytotoxicity in H9c2 cells as detected by LDH assay, suggesting that D006 at the testing concentrations (1 μM, 3 μM, and 10 μM) used is not cytotoxic. Dox (1 μM) treatment for 24 h markedly decrease cell viability and increased LDH release, while co-treatment with D006 protected cell viability and reduced LDH release in a dose-dependent manner (Fig. 2B and 2C). The protective effects of D006 and its parental compounds, against Dox-induced toxicity in H9c2 cells, were also investigated. Figure 2D illustrates that D006 (10 μM) was much more effective than DSS (10 μM), TMP (10 μM), ACS (10 μM), DSS+TMP+ACS, ADTM (10 μM) and ADTM + ACS in preventing Dox-induced cell injury in H9c2 cells. D006 also protected against Dox-induced toxicity in differentiated H9c2 cells (Fig. 2E). Co-treatment with D006 and Dox increased ATP levels and mitochondrial membrane potential in H9c2 cells when compared to Dox-treated group (Fig. 2F and Supplementary Figure S1). Furthermore, representative images of F-actin indicate that D006 treatment preserved Dox-induced morphological changes in H9c2 cells (Fig. 3A). Dox-induced cardiotoxicity, via promotion of ROS expression, and dysfunction in the mitochondria of cardiomyocytes, has been reported [Green and Leeuwenburgh, 2002]. To examine whether D006 attenuated ROS after Dox treatment, H9c2 cells were treated with Dox (1 μM) in the presence or absence of D006 (10 μM) for 24 h, after loading with the ROS indicator DCFH-DA. As shown in Figure 3B, exposing H9c2 cells to Dox resulted in greater ROS augmentation compared to control cells, while co-treatment with D006 (10 μM) significantly attenuated ROS levels after 24 h incubation. D006 treated alone had no effects on ROS generation. The proportion of apoptotic cells (with changes in chromatin condensation) was increased after Dox treatment for 24 h when compared to the control group, in which apoptotic cell expression significantly reduced after co-treatment with Dox and D006 (Fig. 3C).

D006 PROMOTED MITOCHONDRIAL BIOGENESIS IN H9c2 CELLS.

To investigate the effects of D006 on the expression of PGC-1α protein, H9c2 cells were treated with D006 for different time periods. Figure 4A and B illustrates that D006 upregulated expression of PGC-1α protein. The expression of PGC-1β and Tfam mRNA, both of which regulate mitochondrial biogenesis, was significantly increased after 24 h of D006 treatment, as detected by RT-PCR (Fig. 4C and D). Mitochondrial function was increased after D006 treatment as showed by enhanced MTT reduction (Fig. 4E). Representative images demonstrate that D006 treatment increased the number of mitochondria and promoted the nuclear translocation of NRF-1 proteins (Supplementary Figure S2 and Fig. 4F). Taken together, these data indicate that D006 treatment may stimulate mitochondrial biogenesis in H9c2 cells.

D006 RESTORED MITOCHONDRIAL BIOGENESIS AND mtDNA COPY NUMBER AFTER DOXORUBICIN TREATMENT IN H9c2 CELLS

The expression of mRNA levels of regulators during mitochondrial biogenesis in H9c2 cells was analyzed after 24 h of Dox treatment in the presence or absence of D006. The expression of PGC-1α, PGC-1β and Tfam mRNA was significantly decreased after 24 h of Dox treatment (Supplementary Figure S3). These results indicate that mitochondrial biogenesis was disturbed by Dox in H9c2 cells. To investigate whether D006 may prevent the inhibition of mitochondrial biogenesis induced by Dox, the expression of PGC-1α, NRF-1 and Nrf2 proteins were detected by Western blot. Dox decreased the protein levels of PGC-1α, NRF-1 and Nrf2 (Fig. 5A). Densitometric analysis showed D006 treatment increased the expression of NRF-1 (Fig. 5B), PGC-1α (Fig. 5C), and Nrf2 (Fig. 5D) proteins after Dox treatment. To investigate whether D006 protects against Dox-induced mtDNA damage in H9c2 cells, mtDNA copy numbers were measured by RT-PCR. After Dox treatment, the

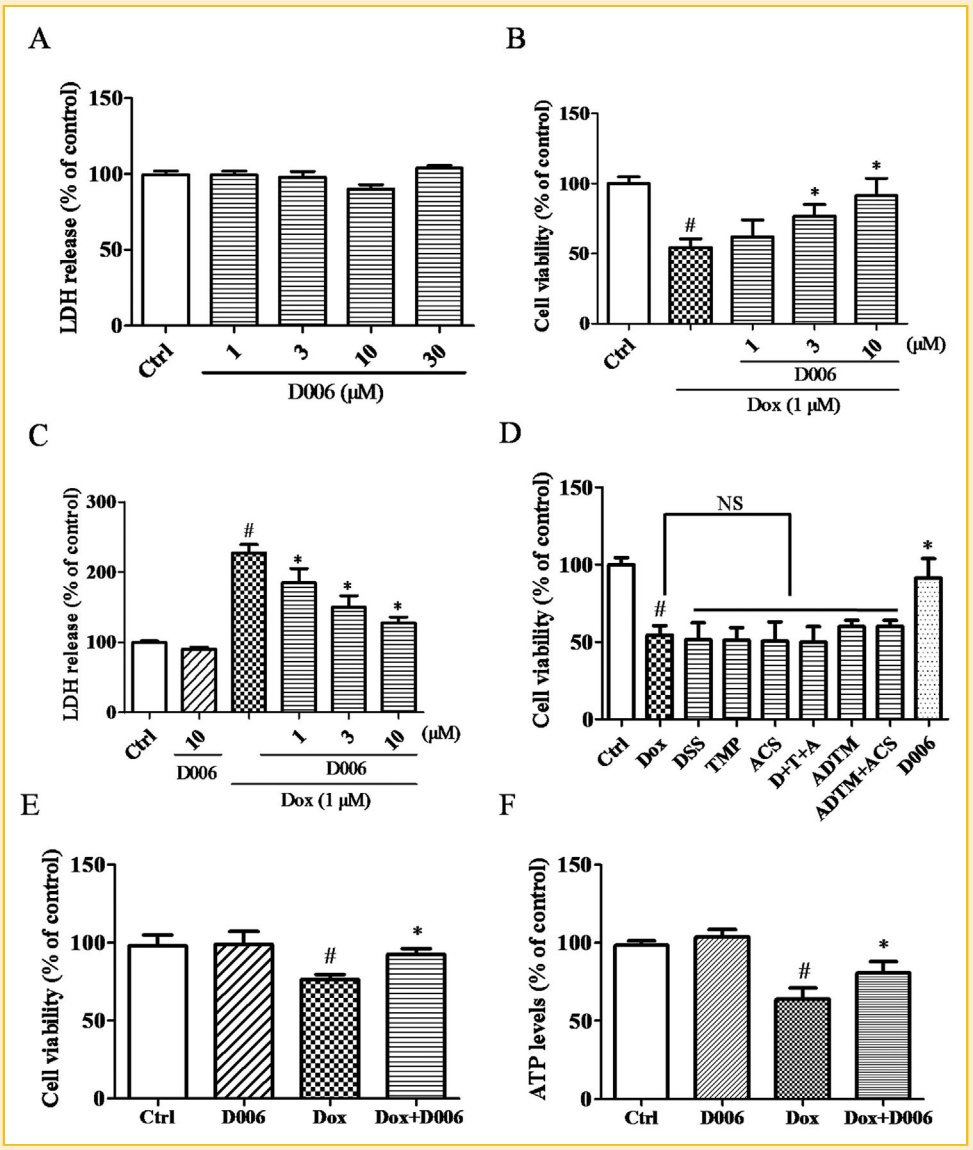

Fig. 2. D006 protected against doxorubicin-induced cell injury in H9c2 cells. (A) H9c2 cells were treated with different concentrations of D006 for 24 h. The cytotoxicity of H9c2 cells was measured by lactate dehydrogenase (LDH) assay. The viability (B) and toxicity (C) of H9c2 cells were determined after 24 h Dox treatment (1 μM) in the presence or absence of different concentrations of D006. Cell viability was examined by MTT assay. (D) Treatment with DSS, TMP, ACS, D + T + A (DSS + TMP + ACS), ADTM and ADTM + ACS did not attenuate Dox-induced cell injury. (E) D006 protected against Dox-induced toxicity in differentiated H9c2 cells. (F) D006 preserved ATP levels in H9c2 cells after Dox treatment. NS, non-significant; $^{\#}P < 0.05$ versus Ctrl and $^{*}P < 0.05$ versus Dox; n = 3.

mtDNA level decreased by 64.8% compared to control cells. In contrast, co-treatment with D006 suppressed Dox-induced loss of mtDNA copy numbers of H9c2 cells compared to Dox alone (Fig. 6D).

D006 PROTECTED AGAINST DOX-INDUCED APOPTOSIS AND mtDNA DAMAGE VIA HO-1

Previous studies have shown that overexpression of the antioxidant enzyme HO-1 protects against Dox induced apoptosis and mtDNA damage in cardiomyocytes [Suliman et al., 2007a]. To investigate the effects of D006 on the expression of HO-1 protein, H9c2 cells were treated with D006 (10 μM) for different time periods. As shown in Figure 6A, D006 upregulated the expression of HO-1 protein in a time-dependent manner. Known down of HO-1 by siRNA reversed the protective effect of D006 against Dox-induced toxicity in H9c2 cells (Fig. 6B). The activity of caspase-3 in H9c2 cells significantly increased after 24 h of treatment with Dox, which was inhibited by co-treatment with Dox and D006 (Fig. 6C). Furthermore, pre-treatment with the HO-1 inhibitor zinc protoporphyrin (Znpp), at 5 μM for 30 min, abolished the inhibitory effects of D006 on the caspase-3 activity induced by Dox. Treatment with D006 or Znpp alone had no effect on basal caspase-3 activity compared to the control group, which was further confirmed by the results of Western blot of cleaved-caspase 9 and cleaved-PARP proteins (Fig. 6C). D006

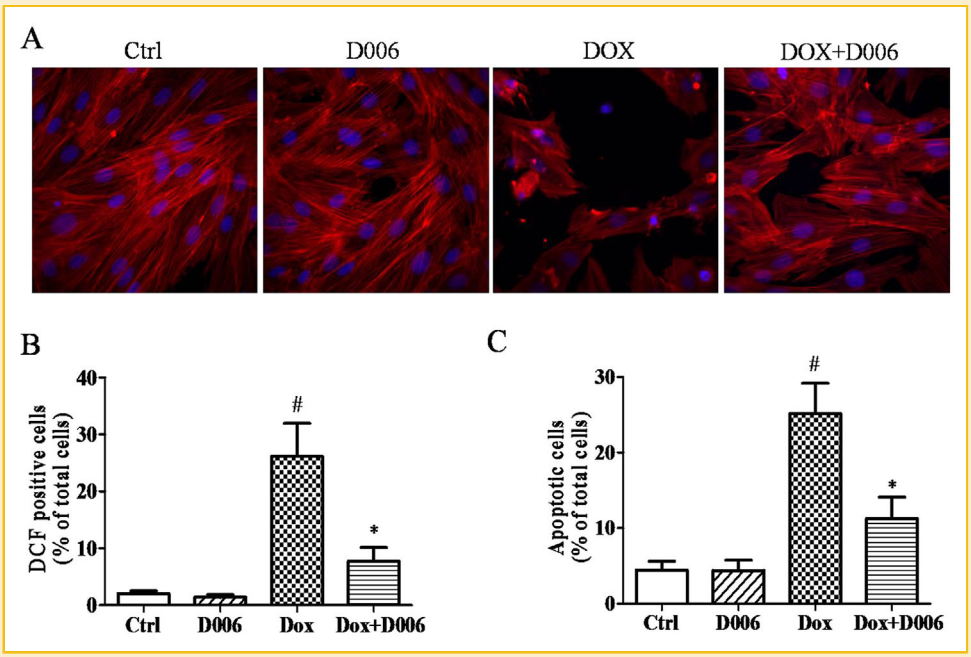

Fig. 3. Effects of D006 on changes in morphology, ROS generation and cell apoptosis in H9c2 cells. (A) Cell morphology in H9c2 cells was measured by immunostaining. F-actin and H9c2 nuclei were stained with rhodamine phalloidin and DAPI, respectively. (B) The percentage of DCFH-DA staining cells after 24 h of Dox with or without D006 treatment in H9c2 cells. (C) The percentage of apoptotic cells after 24 h of Dox with or without D006 treatment in H9c2 cells. Apoptotic cells were detected by Hoechst 33342 staining. Doxorubicin treatment for 24 h elevated the number of ROS-positive and apoptotic cells while co-retreatment with D006 significantly decreased the number of DCFH-DA positive cells and apoptotic cells after treatment with Dox. $^{\#}P < 0.05$ versus Ctrl and $^{*}P < 0.05$ versus Dox; n = 3.

protection against Dox-induced mtDNA damage, via HO-1, was also confirmed using the HO-1 inhibitor Znpp. Pretreatment with Znpp for 30 min before Dox treatment attenuated the protective effects of D006 as shown by the mtDNA copy number. Znpp alone did not change the mtDNA copy number in H9c2 cells (Fig. 6D). D006 suppressed Dox-induced cell apoptosis and mtDNA depletion in H9c2 cells through an HO-1-dependent pathway.

D006 PROTECTED AGAINST DOX-INDUCED CARDIOTOXICITY IN ZEBRAFISH

The protective effects of D006 against cardiotoxicity mediated by Dox in zebrafish were quantified. As shown in Figure 7, Dox treatment for 32 h significantly decreased the heat rate and cardiac function of zebrafish, indicated by stroke volume, cardiac output and percentage of fractional shortening (% FS). The representative images in Figure 7A indicate that the systolic and diastolic function of the ventricle was damaged after Dox treatment, which was partly recovered by D006. D006 and DSS preserved Dox-induced heart rate decreases in zebrafish (Fig. 7B). Furthermore, D006 at 30 μM significantly restored stroke volume, cardiac output and % FS after Dox treatment and D006 alone did not affect the cardiac function of zebrafish (Fig. 7C–E). However, DSS (30 μM) treatment did not significantly maintain cardiac function after Dox treatment in zebrafish.

D006 ENHANCED DOX-INDUCED CELL APOPTOSIS IN BREAST CANCER CELLS

The effects of Dox and D006 on cell death in MFC-7 cells were evaluated. Figure 8A shows that the number of viable MCF-7 cells was reduced after 24 h of Dox (1 μM) treatment. Co-treatment with Dox and D006 further enhanced cytotoxicity in MCF-7 cells. D006 alone had no effect on the number of MCF-7 cells. Our data suggest that combined D006 and Dox treatment confers a synergistic effect against Dox-induced cell death in MCF-7 cells. The expression of p53, p-p53^{ser15} and other apoptotic-related proteins such as cleaved-caspase 9 and cleaved-PARP in MCF-7 cells were examined by Western blot. As shown in Figure 8B, after Dox treatment for 24 h, the expression of p53, p-p53^{ser15}, cleaved-caspase 9 and cleaved-PARP proteins was elevated in MCF-7 cells. Similarly, the expression of these proteins was further increased after Dox and D006 co-treatment.

DISCUSSION

In this study, the novel compound D006 was synthesized, derived from coupling the structures of DSS, TMP and ACS. DSS, a major active ingredient of the Chinese medicinal herb Danshen, displays many potentially cardioprotective effects such as inhibition of platelet aggregation, promotion of microcirculation and protection against ischemia/reperfusion injury in myocardium both in vivo and in vitro [Cui et al., 2013; Yin et al., 2013]. On the other hand, TMP, which is isolated from another Chinese herb, Chuanxiong, exhibited a number of protective effects including reducing ischemic brain injury and anti-apoptotic effects against spinal cord ischemia in vivo, protection against hydrogen peroxide and iron-induced oxidative injury and inhibition of platelet aggregation [Fan et al., 2006; Li et al., 2010; Cui et al., 2013]. Previous studies indicate that

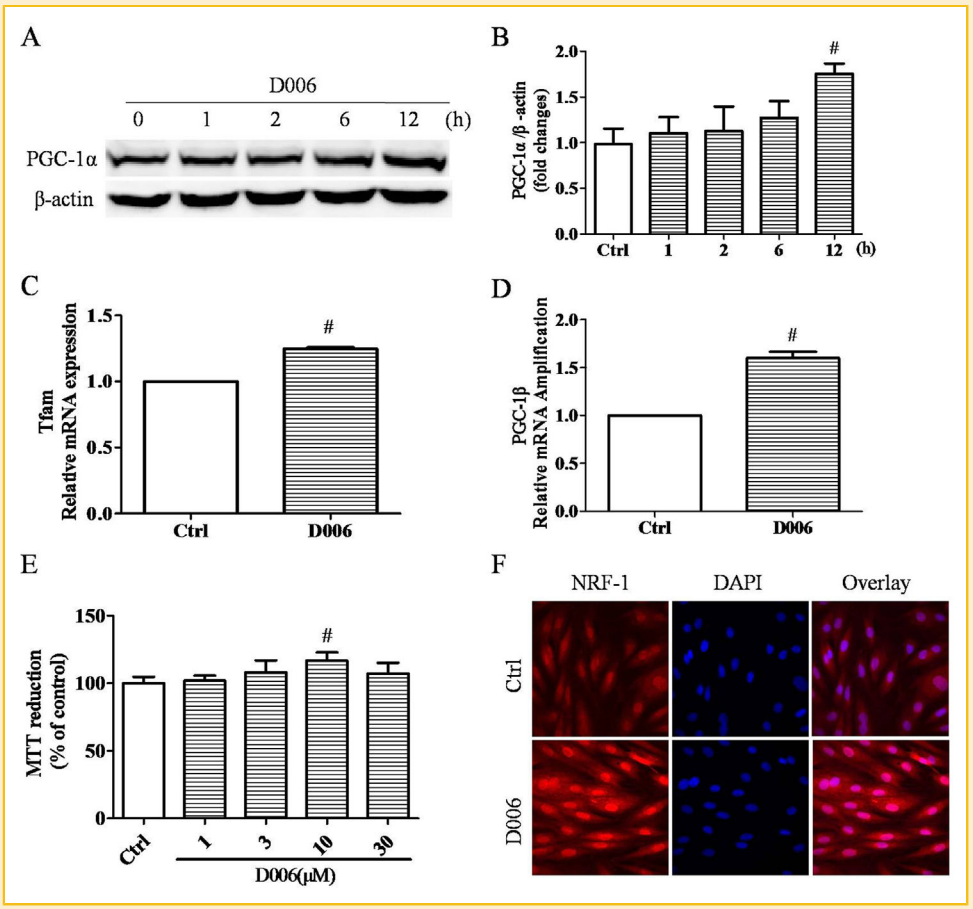

Fig. 4. D006 promoted mitochondrial biogenesis in H9c2 cells. (A, B) D006 increased the expression of PGC-1α protein, as measured by Western blot. The expression of Tfam (C) and PGC-1β (D), regulators of mitochondrial biogenesis, was detected by RT-PCR. (E) H9c2 cells were treated with different concentration of D006 for 24 h, MTT reduction was detected by MTT assay. (F) Nuclear translocation of NFR-1 proteins was determined by immunofluorescence staining. $^{\#}P < 0.05$ versus Ctrl.

ACS can release H_2S into the circulation, which confers cardioprotection against myocardial ischemia in mice and Dox-induced cardiotoxicity in H9c2 cells [Calvert et al., 2009; Guo et al., 2013b].

In our previous study, ADTM, a DSS-TMP conjugate, conferred cardioprotection against t-BHP-induced cell injury in vitro and acute myocardial ischemia in vivo [Cui et al., 2013]. However, ADTM was not sufficiently potent to protect against Dox-induced cardiotoxicity in H9c2 cells and it was unstable in vivo due to the weak ester bond between TMP and DSS [Li et al., 2015]. Based on these studies, another novel DSS derivative, D006, a high sterically hindered conjugate of DSS, TMP and the H_2S donor ACS, was synthesized to improve the stability and cardioprotective effects of ADTM by combining ADTM and ACS. D006 was approximately 30-fold more potent than ADTM in ameliorating Dox-induced cardiotoxicity and t-BHP induced cell injury in H9c2 cells (unpublished data). Moreover, D006, but not single or combined treatment with DSS, TMP, ACS, or ADTM, conferred cardioprotection against Dox-induced cardiotoxicity in H9c2 cells.

ROS production in response to Dox in cardiomyocytes plays an important role in Dox-induced cardiotoxicity. According to the ROS hypothesis, Dox-induced ROS increases in the presence of ion, which leads to damage to DNA and proteins, lipid peroxidation and eventual myocyte death [Sawyer, 2013; Ichikawa et al., 2014]. Previous studies suggest that Dox may trigger apoptosis in cardiomyocytes and activation of caspase 3, caspase 9 and cleaved-PARP, all of which are the executioners of apoptosis induced by Dox. Berberine protected against Dox-induced cardiotoxicity and inhibited the activity of caspase 3 and caspase 9 after Dox treatment in cardiomyocytes. Dox increased the expression of cleaved-caspase 3, caspase 9 and PARP proteins in H9c2 cells and rat heart tissues, which were decreased after isorhamnetin treatment [Lv et al., 2012; Sun et al., 2013a]. In the present study, D006 reduced ROS generation mediated by Dox in H9c2 cells. Furthermore, Dox and D006 treatment decreased the activity of caspase-3 activated by Dox. In addition, Dox increased the expression of cleaved-caspase-3, 9 and PARP proteins in H9c2 cells, which was inhibited by D006 treatment. Alterations in the cell morphology of H9c2 cells were analyzed by F-actin staining. The data showed that D006 also preserved changes in cell morphology after Dox treatment.

Mitochondrial biogenesis depends on the expression of PGC-1, NRF-1, Nrf2 and Tfam proteins and requires the participation of genomes in nuclear and mitochondria [Sharma et al., 2014].

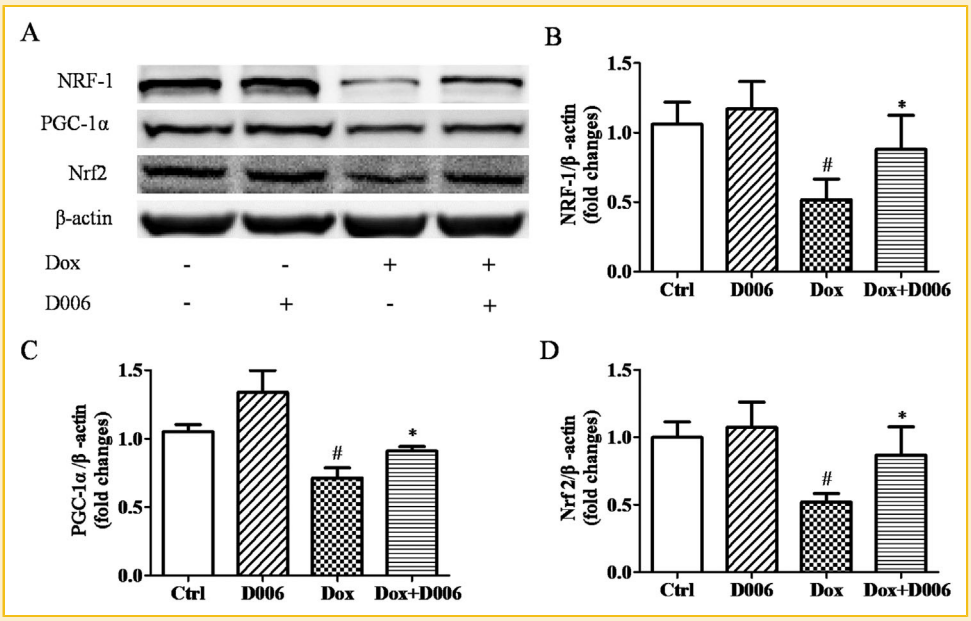

Fig. 5. D006 restored mitochondrial biogenesis after doxorubicin treatment in H9c2 cells. (A) The expression of NRF-1, PGC-1α and Nrf2 proteins, regulators of mitochondrial biogenesis, was measured by Western blot as compared with β-actin. (B–D) The expression of NRF-1, PGC-1α and Nrf2 proteins was analyzed by densitometric quantification. $^{\#}P < 0.05$ versus Ctrl and $^{*}P < 0.05$ versus Dox; n = 3.

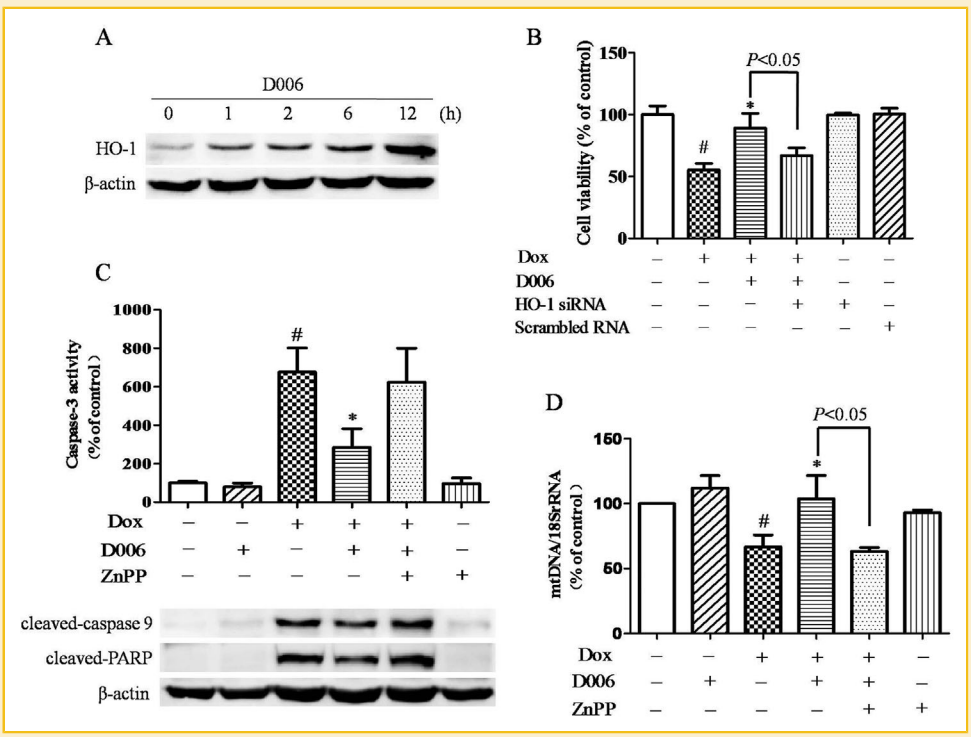

Fig. 6. D006 protected against Dox-induced apoptosis and mtDNA damage via HO-1. (A) The time course of HO-1 protein expression was detected by Western blot after D006 treatment in H9c2 cells. (B) Knowndown of HO-1 by siRNA reversed the protective effect of D006 against Dox-mediated cardiotoxicity in H9c2 cells. (C) Histogram indicating caspase-3 activity, determined by Caspase-3 Activity Assay. The results were consistent with that of cleaved-caspase 9 and cleaved-PARP as shown below the histogram. (D) D006 decreased doxorubicin-induced mtDNA depletion via HO-1. The histogram indicates that H9c2 cells were pretreated with Znpp for 30 min and then treated with doxorubicin with or without D006, and with D006 alone. The mtDNA copy number decreased after doxorubicin treatment, which was inhibited by D006. Pre-treatment with Znpp abolished the protective effects of D006. $^{\#}P < 0.05$ versus Ctrl and $^{*}P < 0.05$ versus Dox; n = 3.

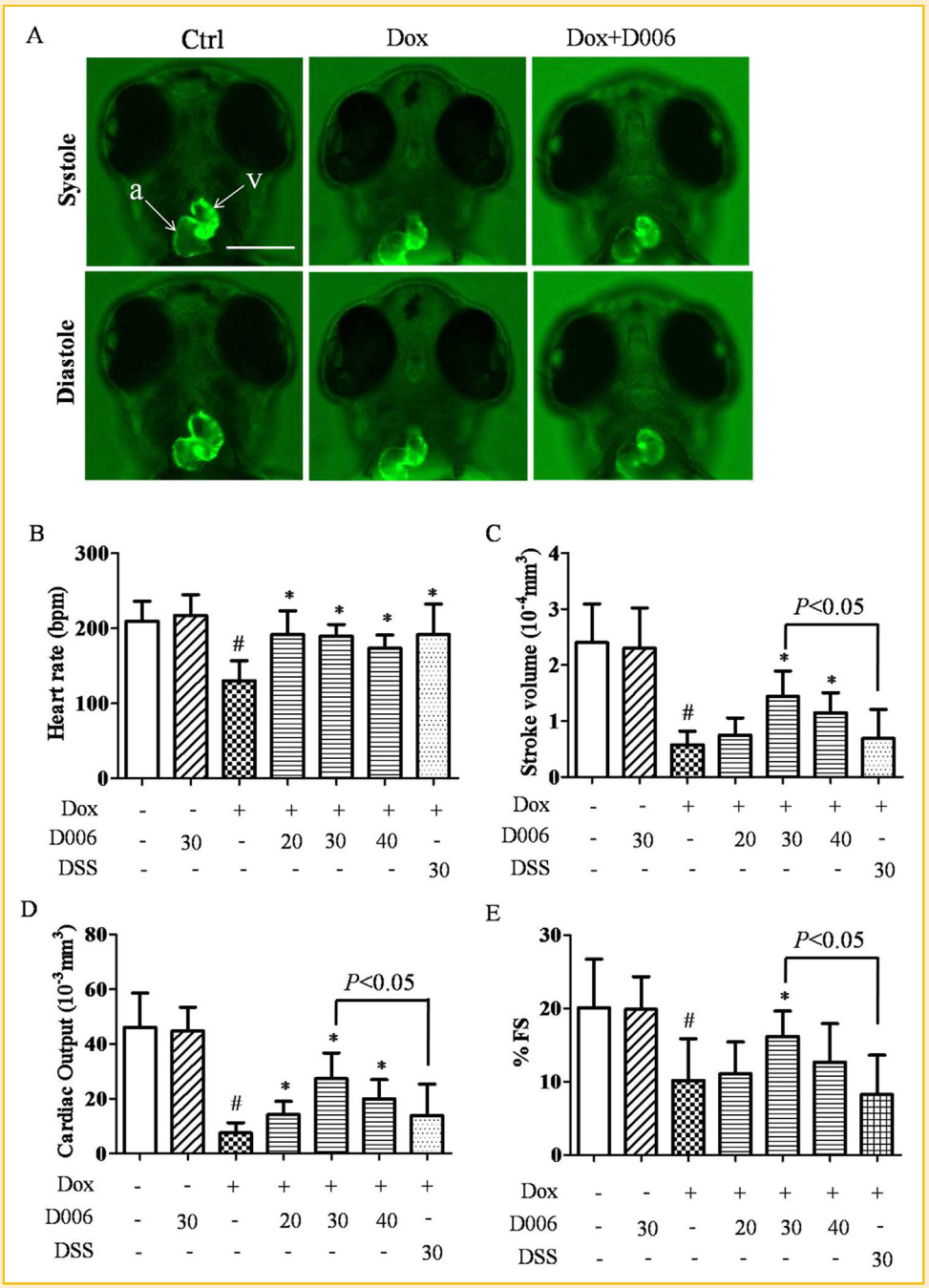

Fig. 7. D006 protected against the loss of ventricular function mediated by Dox in zebrafish. (A) Representative images of zebrafish heart after treatment with Dox in the presence or absence of D006, a: Atrium, v: Ventricle. Scale bar: 200 μm. Zebrafish were co-treated with DSS, D006, and Dox, the changes in heart rate (B), stroke volume (C), cardiac output (D) and % FS (E) were measured. $^{\#}P < 0.05$ versus Ctrl and $^{*}P < 0.05$ versus Dox; n = 3.

Evidence suggests that preservation of mitochondrial biogenesis in cardiomyocytes plays an essential role in cardioprotection. Acetylcholine protected against hypoxia/reoxygenation induced cell injury through increasing mitochondrial biogenesis [Sun et al., 2013b]. Mitochondrial biogenesis and mtDNA in cardiomyocytes were suppressed after Dox treatment both in vivo and in vitro, which is the main pathogenesis of Dox-induced cardiotoxicity [Suliman et al., 2007; Miyagawa et al., 2010; Bouitbir et al., 2012]. Metallothionein conferred cardioprotective effects against Dox-induced cardiotoxicity in mice by preserving mitochondrial biogenesis [Guo et al., 2014]. Endothelin-converting enzyme-1 (ECE-1) inhibition reduced the impairment of cardiac mitochondrial biogenesis, which protected against Dox-induced cardiomyopathy [Miyagawa et al., 2010]. Carbon monoxide (CO) treatment promotes mitochondrial biogenesis both in vivo and in vitro [Suliman et al., 2007]. The CO/heme oxygenase (HO) system also

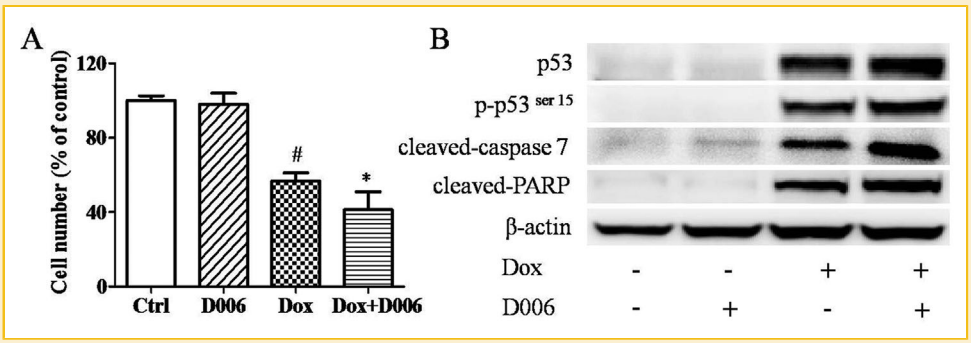

Fig. 8. D006 enhanced Dox-induced cell death in MCF-7 breast cancer cells. (A) Number of MCF-7 cells after Dox and D006 treatment for 24 h. (B) The expression of p53, p-p53^{ser15}, cleaved-caspase 9 and cleaved-PARP proteins was detected by Western blot. MCF-7 cells were treated with Dox (1 μM) for 24 h with or without D006 (10 μM). $^{\#}P < 0.05$ versus Ctrl and $^{*}P < 0.05$ versus Dox; n = 3.

prevents Dox-induced cardiotoxicity through the promotion of cardiac mitochondrial biogenesis and mtDNA copy numbers [Suliman et al., 2007a; Piantadosi et al., 2008]. Another study showed that atovastatin, through ROS-mediated mitochondrial biogenesis, improved antioxidant activity in the heart and preserved mitochondrial membrane potential in H9c2 cells after Dox treatment [Bouitbir et al., 2012]. Our study confirms that Dox significantly decreases levels of PGC-1α, PGC-1β and Tfam mRNA as well as the copy numbers of mtDNA in H9c2 cells. Dox treatment in H9c2 cells decreased the expression of PGC-1α, NRF-1 and Nrf-2 proteins, which was restored by D006. Furthermore, D006 increased the expression of PGC-1β and Tfam mRNA, promoting MTT reduction as well as the nuclear translocation of NRF-1 proteins. The numbers of mitochondria in H9c2 cells were also increased after D006 treatment. These data suggest that the signal pathway of mitochondrial biogenesis may be involved in the cardioprotection conferred by D006.

Accumulating evidence indicates that HO-1 offers cardioprotection against Dox-induced cardiotoxicity [Piantadosi et al., 2008; Kim et al., 2009]. HO-1 promoted mitochondrial biogenesis and increased mtDNA numbers after Dox treatment, which opposed Dox-mediated toxicity [Suliman et al., 2007a; Piantadosi et al., 2008]. In the present study, D006 promoted the expression of the HO-1 protein in a time-dependent manner in H9c2 cells. The protective effect of D006 on Dox-induced cell death was significantly reversed after HO-1 knockdown using HO-1 siRNA. Further study showed that pretreatment with the HO-1 inhibitor Znpp resulted in increased caspase-3 activity and pro-apoptotic protein expression in Dox/D006-treated cells. Similarly, D006 attenuated Dox-induced loss of mtDNA copy number, which was reversed by pretreatment with Znpp. Taken together, our results suggest that D006, through the HO-1 pathway, protects against Dox-induced cardiotoxicity by preserving the copy number of mtDNA.

Zebrafish models are widely used to assess cardiotoxicity in preclinical studies. Previous study showed that sorafenib decreases the number of ventricular cardiomyocytes and promotes cardiomyocyte apoptosis in zebrafish [Cheng et al., 2011]. After 72 h of clostridium difficile toxin B treatment, the cardiac function of zebrafish deteriorated, which included reductions in heart rate and blood flow, changes in ventricular morphology and the loss of ventricular contraction [Hamm et al., 2006]. In our study, the protective effects of D006 against Dox-induced cardiotoxicity were tested in zebrafish: Dox treatment significantly decreased stroke volume, cardiac output and the percentage of fractional shortening (% FS) when compared to the untreated group. Changes in ventricular function, mediated by Dox in zebrafish, were observed, similar to changes in a previous Dox-induced mice/rat model in vivo [Riad et al., 2009; Miyagawa et al., 2010]. In our study D006, but not DSS, maintained the stroke volume, cardiac output and FS % of zebrafish after Dox treatment.

We also explored the effect of D006 on the chemotherapeutic efficacy of Dox. The results showed that the numbers of MCF-7 cells were reduced after Dox treatment, which were further decreased by D006 co-treatment. D006 alone had no effects on the viability of MCF-7 cells. This was consistent with results showing that D006 enhanced the expression of p53, p-p53 and pro-apoptotic proteins such as cleaved-caspase 7 and cleaved-PARP in MCF-7 cells after Dox treatment. D006 also boosted Dox-induced ROS generation in MCF-7 cells (data not shown). ROS may promote DNA damage in cells, leading to the activation of p53 proteins that play a vital role in promoting cancer cell apoptosis [Wang et al., 2004; Liu et al., 2013]. Therefore, it was postulated that D006 would enhance Dox-induced cell apoptosis through p53 activation.

It has been reported that the expression of PGC-1α is decreased in many kinds of cancers, such as breast, ovarian and colon cancer [Onishi et al., 2014]. Overexpression of PGC-1α promotes cell apoptosis in musculoskeletal malignancies and human epithelial ovarian cancer cells [Zhang et al., 2007; Onishi et al., 2014]. The anti-proliferative and pro-apoptotic activity of 5′-deoxy-5-fluorouridine in breast and colon cancer cells was enhanced by PGC-1α [Kong et al., 2009]. PGC-1α also potentiated the anti-cancer effects of doxorubicin in breast cancer cells [Skildum et al., 2011]. In our study, D006 significantly increased the expression of PGC-1α mRNA (data not shown) in MCF-7 cells. Therefore, D006 may act through PGC-1α to promote the anticancer effects of Dox in breast cancer cells. However, the potential mechanism underlying the synergistic anticancer effects generated by D006 and Dox in MCF-7 cells requires further investigation.

In conclusion, D006 displayed cardioprotective effects against Dox-induced cardiotoxicity both in vivo and in vitro. The potential mechanisms underlying D006-induced cardioprotection may be mediated by the preservation of mitochondrial biogenesis and promotion of HO-1 protein expression. D006 also potentiated the chemotherapeutic efficacy of Dox in MCF-7 breast tumor cells via p53 activation. These findings suggest that D006 represents a promising novel agent for the amelioration of cardiac toxicity, such that potentiating the chemotherapeutic efficacy of Dox merits further investigation.

REFERENCES

Bouitbir J, Charles AL, Echaniz-Laguna A, Kindo M, Daussin F, Auwerx J, Piquard F, Geny B, Zoll J. 2012. Opposite effects of statins on mitochondria of cardiac and skeletal muscles: A 'mitohormesis' mechanism involving reactive oxygen species and PGC-1. Eur Heart J 33: 1397–1407.

Calvert JW, Jha S, Gundewar S, Elrod JW, Ramachandran A, Pattillo CB, Kevil CG, Lefer DJ. 2009. Hydrogen sulfide mediates cardioprotection through Nrf2 signaling. Circ Res 105:365–U105.

Cheng H, Kari G, Dicker AP, Rodeck U, Koch WJ, Force T. 2011. A novel preclinical strategy for identifying cardiotoxic kinase inhibitors and mechanisms of cardiotoxicity. Circ Res 109:1401–1409.

Cui G, Shan L, Hung M, Lei S, Choi I, Zhang Z, Yu P, Hoi P, Wang Y, Lee SM. 2013. A novel danshensu derivative confers cardioprotection via PI3K/Akt and Nrf2 pathways. Int J Cardiol 168:1349–1359.

Ding Y, Sun X, Huang W, Hoage T, Redfield M, Kushwaha S, Sivasubbu S, Lin X, Ekker S, Xu X. 2011. Haploinsufficiency of target of rapamycin attenuates cardiomyopathies in adult zebrafish. Circ Res 109:658–669.

Fan LH, Wang KZ, Cheng B, Wang CS, Dang XQ. 2006. Anti-apoptotic and neuroprotective effects of tetramethylpyrazine following spinal cord ischemia in rabbits. BMC Neurosci 7:48.

Feenstra J, Grobbee DE, Remme WJ, Stricker BHC. 1999. Drug-induced heart failure. J Am Coll Cardiol 33:1152–1162.

Gharib MI, Burnett AK. 2002. Chemotherapy-induced cardiotoxicity: Current practice and prospects of prophylaxis. Eur J Heart Fail 4:235–242.

Green PS, Leeuwenburgh C. 2002. Mitochondrial dysfunction is an early indicator of doxorubicin-induced apoptosis. Biochim Biophys Acta 1588: 94–101.

Guo RM, Lin JC, Xu WM, Shen N, Mo LQ, Zhang CR, Feng JQ. 2013a. Hydrogen sulfide attenuates doxorubicin-induced cardiotoxicity by inhibition of the p38 MAPK pathway in H9c2 cells. Int J Mol Med 31:644–650.

Guo RM, Wu K, Chen JF, Mo LQ, Hua XX, Zheng DD, Chen PX, Chen G, Xu WM, Feng JQ. 2013b. Exogenous hydrogen sulfide protects against doxorubicin-induced inflammation and cytotoxicity by inhibiting p38MAPK/NF kappa B pathway in H9c2 cardiac cells. Cell Physiol Biochem 32:1668–1680.

Guo J, Guo Q, Fang H, Lei L, Zhang T, Zhao J, Peng S. 2014. Cardioprotection against doxorubicin by metallothionein is associated with preservation of mitochondrial biogenesis involving PGC-1alpha pathway. Eur J Pharmacol 737:117–124.

Hamm EE, Voth DE, Ballard JD. 2006. Identification of Clostridium difficile toxin B cardiotoxicity using a zebrafish embryo model of intoxication. Proc Natl Acad Sci USA 103:14176–14181.

Huang CJ, Tu CT, Hsiao CD, Hsieh FJ, Tsai HJ. 2003. Germ-line transmission of a myocardium-specific GFP transgene reveals critical regulatory elements in the cardiac myosin light chain 2 promoter of zebrafish. Dev Dyn 228: 30–40.

Huang W, Deng Y, Dong W, Yuan WZ, Wan YQ, Mo XY, Li YQ, Wang ZQ, Wang YQ, Ocorr K, Zhang B, Lin S, Wu XS. 2011. The effect of excess expression of GFP in a novel heart-specific green fluorescence zebrafish regulated by nppa enhancer at early embryonic development. Mol Biol Rep 38:793–799.

Ichikawa Y, Ghanefar M, Bayeva M, Wu RX, Khechaduri A, Prasad SVN, Mutharasan RK, Naik TJ, Ardehali H. 2014. Cardiotoxicity of doxorubicin is mediated through mitochondrial iron accumulation. J Clin Invest 124: 617–630.

Kim DS, Chae SW, Kim HR, Chae HJ. 2009. CO and bilirubin inhibit doxorubicin-induced cardiac cell death. Immunopharmacol Immunotoxicol 31:64–70.

Kong X, Fan H, Liu X, Wang R, Liang J, Gupta N, Chen Y, Fang F, Chang Y. 2009. Peroxisome proliferator-activated receptor gamma coactivator-1alpha enhances antiproliferative activity of 5′-deoxy-5-fluorouridine in cancer cells through induction of uridine phosphorylase. Mol Pharmacol 76: 854–860.

Li S, Shan L, Zhang Z, Li W, Liao K, Sheng X, Yu P, Wang Y. 2015. Pharmacokinetic and metabolic studies of ADTM: A vovel Danshensu derivative confers cardioprotection by HPLC-UV and LC-MS/MS. J Chromatogr Sci 53:872–878.

Li WM, Liu HT, Li XY, Wu JY, Xu G, Teng YZ, Ding ST, Yu C. 2010. The effect of tetramethylpyrazine on hydrogen peroxide-induced oxidative damage in human umbilical vein endothelial cells. Basic Clin Pharmacol Toxicol 106:45–52.

Liu C, Liu Z, Li M, Li X, Wong YS, Ngai SM, Zheng W, Zhang Y, Chen T. 2013. Enhancement of auranofin-induced apoptosis in MCF-7 human breast cells by selenocystine, a synergistic inhibitor of thioredoxin reductase. PLoS ONE 8:e53945.

Lv X, Yu X, Wang Y, Wang F, Li H, Lu D, Qi R, Wang H. 2012. Berberine inhibits doxorubicin-triggered cardiomyocyte apoptosis via attenuating mitochondrial dysfunction and increasing Bcl-2 expression. PLoS ONE 7: e47351.

Marutani E, Kosugi S, Tokuda K, Khatri A, Nguyen R, Atochin DN, Kida K, Van Leyen K, Arai K, Ichinose F. 2012. A novel hydrogen sulfide-releasing N-methyl-D-aspartate receptor antagonist prevents ischemic neuronal death. J Biolog Chem 287:32124–32135.

Misset JL, Dieras V, Gruia G, Bourgeois H, Cvitkovic E, Kalla S, Bozec L, Beuzeboc P, Jasmin C, Aussel JP, Riva A, Azli N, Pouillart P. 1999. Dose-finding study of docetaxel and doxorubicin in first-line treatment of patients with metastatic breast cancer. Ann Oncol 10:553–560.

Miyagawa K, Emoto N, Widyantoro B, Nakayama K, Yagi K, Rikitake Y, Suzuki T, Hirata K. 2010. Attenuation of Doxorubicin-induced cardiomyopathy by endothelin-converting enzyme-1 ablation through prevention of mitochondrial biogenesis impairment. Hypertension 55:738–746.

Onishi Y, Ueha T, Kawamoto T, Hara H, Toda M, Harada R, Minoda M, Kurosaka M, Akisue T. 2014. Regulation of mitochondrial proliferation by PGC-1alpha induces cellular apoptosis in musculoskeletal malignancies. Sci Rep 4:3916.

Piantadosi CA, Carraway MS, Babiker A, Suliman HB. 2008. Heme oxygenase-1 regulates cardiac mitochondrial biogenesis via Nrf2-mediated transcriptional control of nuclear respiratory factor-1. Circ Res 103: 1232–U1260.

Riad A, Bien S, Westermann D, Becher PM, Loya K, Landmesser U, Kroemer HK, Schultheiss HP, Tschope C. 2009. Pretreatment with statin attenuates the cardiotoxicity of Doxorubicin in mice. Cancer Res 69:695–699.

Sawyer DB. 2013. Anthracyclines and heart failure. N Engl J Med 368: 1154–1156.

Sharma J, Johnston MV, Hossain MA. 2014. Sex differences in mitochondrial biogenesis determine neuronal death and survival in response to oxygen glucose deprivation and reoxygenation. BMC Neurosci 15:9.

Skildum A, Dornfeld K, Wallace K. 2011. Mitochondrial amplification selectively increases doxorubicin sensitivity in breast cancer cells with acquired antiestrogen resistance. Breast Cancer Res Treat 129:785–797.

Suliman HB, Carraway MS, Ali AS, Reynolds CM, Welty-Wolf KE, Piantadosi CA. 2007a. The CO/HO system reverses inhibition of mitochondrial biogenesis and prevents murine doxorubicin cardiomyopathy. J Clin Invest 117:3730–3741.

Suliman HB, Carraway MS, Tatro LG, Piantadosi CA. 2007b. A new activating role for CO in cardiac mitochondrial biogenesis. J Cell Sci 120:299–308.

Sun J, Sun G, Meng X, Wang H, Luo Y, Qin M, Ma B, Wang M, Cai D, Guo P, Sun X. 2013a. Isorhamnetin protects against doxorubicin-induced cardiotoxicity in vivo and in vitro. PLoS ONE 8:e64526.

Sun L, Zhao M, Yu XJ, Wang H, He X, Liu JK, Zang WJ. 2013b. Cardioprotection by acetylcholine: A novel mechanism via mitochondrial biogenesis and function involving the PGC-1alpha pathway. J Cell Physiol 228:1238–1248.

Swain SM, Vici P. 2004. The current and future role of dexrazoxane as a cardioprotectant in anthracycline treatment: Expert panel review. J Cancer Res Clin Oncol 130:1–7.

Swain SM, Whaley FS, Ewer MS. 2003. Congestive heart failure in patients treated with doxorubicin—A retrospective analysis of three trials. Cancer 97:2869–2879.

Tang JY, Li S, Li ZH, Zhang ZJ, Hu GA, Cheang LCV, Alex D, Hoi MPM, Kwan YW, Chan SW, Leung GPH, Lee SMY. 2010. Calycosin promotes angiogenesis involving estrogen receptor and mitogen-activated protein kinase (MAPK) signaling pathway in zebrafish and HUVEC. PloS ONE 5:e11822.

Von Hoff DD, Layard MW, Basa P, Davis HL, Jr., Von Hoff AL, Rozencweig M, Muggia FM. 1979. Risk factors for doxorubicin-induced congestive heart failure. Ann Intern Med 91:710–717.

Wang S, Konorev EA, Kotamraju S, Joseph J, Kalivendi S, Kalyanaraman B. 2004. Doxorubicin induces apoptosis in normal and tumor cells via distinctly different mechanisms. Intermediacy of H(2)O(2)- and p53-dependent pathways. J Biol Chem 279:25535–25543.

Wareski P, Vaarmann A, Choubey V, Safiulina D, Liiv J, Kuum M, Kaasik A. 2009. PGC-1{alpha} and PGC-1{beta} regulate mitochondrial density in neurons. J Biol Chem 284:21379–21385.

Yin Y, Guan Y, Duan J, Wei G, Zhu Y, Quan W, Guo C, Zhou D, Wang Y, Xi M, Wen A. 2013. Cardioprotective effect of Danshensu against myocardial ischemia/reperfusion injury and inhibits apoptosis of H9c2 cardiomyocytes via Akt and ERK1/2 phosphorylation. Eur J Pharmacol 699:219–226.

Zhang Y, Ba Y, Liu C, Sun G, Ding L, Gao S, Hao J, Yu Z, Zhang J, Zen K, Tong Z, Xiang Y, Zhang CY. 2007. PGC-1alpha induces apoptosis in human epithelial ovarian cancer cells through a PPARgamma-dependent pathway. Cell Res 17:363–373.

Zhang YY, Wang CG, Huang LX, Chen R, Chen YX, Zuo ZH. 2012. Low-level pyrene exposure causes cardiac toxicity in zebrafish (Danio rerio) embryos. Aquat Toxicol 114:119–124.

Zhou S, Starkov A, Froberg MK, Leino RL, Wallace KB. 2001. Cumulative and irreversible cardiac mitochondrial dysfunction induced by doxorubicin. Can Res 61:771–777.

SUPPORTING INFORMATION

Additional supporting information may be found in the online version of this article at the publisher's web-site.